

## Domain Wall Motion Across Magnetic and Spin Compensation Points in Magnetic Garnets

M.V. Logunov,<sup>1</sup> S.S. Safonov,<sup>1</sup> A.S. Fedorov,<sup>1,2</sup> A.A. Danilova,<sup>1,2</sup> N.V. Moiseev,<sup>3</sup> A.R. Safin<sup>1,4</sup>,  
S.A. Nikitov<sup>1,2</sup> and A. Kirilyuk<sup>1,5,\*</sup>

<sup>1</sup>*Kotel'nikov Institute of Radio-Engineering and Electronics of RAS, 11-7 Mokhovaya Street, Moscow 125009, Russia*

<sup>2</sup>*Moscow Institute of Physics and Technology, 9 Institutskij Pereulok, Dolgoprudny, Moscow Region 141701, Russia*

<sup>3</sup>*National Research Mordovia State University, 68 Bolshevistskaya Street, Saransk 430005, Russia*

<sup>4</sup>*Moscow Power Engineering Institute, 14 Krasnokazarmennaya Street, Moscow 111250, Russia*

<sup>5</sup>*FELIX Laboratory, Radboud University, Toernooiveld 7, 6525 ED Nijmegen, Netherlands*

(Received 22 November 2020; revised 3 May 2021; accepted 14 May 2021; published 9 June 2021)

Ferrimagnetic materials represent unique systems where the ease of manipulating the spins with applied magnetic fields is combined with exchange-driven acceleration of the internal spin dynamics. Of particular interest is the temperature range around the magnetic and spin compensation points, finely balancing both magnetic moment and angular momentum of the system, and leading to a very particular character of magnetic switching by the domain wall motion. Here we present our studies of the temperature-dependent domain wall dynamics in the temperature range covering both angular momentum and magnetization compensation points in garnet film, and reaching up to the Curie temperature. Drastic difference in the domain wall mobility and maximum achievable velocity in the vicinities of these two compensation points is demonstrated. Also a remarkably high mobility in weak applied magnetic fields is indicated.

DOI: 10.1103/PhysRevApplied.15.064024

### I. INTRODUCTION

Current information technologies use millions of times more energy than is sustainable and radically new disruptive approaches are required to change this situation. It is crucial to find alternative approaches to store and process data in order to reduce information-technology-related energy consumption: efficiency, not scaling, is the issue. Therefore, efficient, local, and fast control of magnetism in ferromagnetic materials is central within current information technologies. Recent years moreover have indicated the potential of antiferromagnetic materials in this area for their fundamentally different and appealing features [1,2]. These are the absence of net magnetization and stray fields eliminating crosstalk between neighboring devices, and the absence of a primary macroscopic magnetization. The associated absence of the related angular momentum, moreover, makes the dynamics in antiferromagnets inherently faster than in ferromagnets [3,4], including that of domain walls (DWs) [5,6]. However, antiferromagnetic order being better shielded from the environment and thus very robust makes it also far more difficult to control and to read out.

As a result of these difficulties, recent years have seen an increase of interest in the dynamics of ferrimagnetic materials, in particular in the motion of DWs [7–10]. In ferrimagnets, a certain freedom exists to manipulate the relative contributions of two sublattices and thus approach the behavior of antiferromagnets. Particular interest is triggered by the vicinity of the point in temperature where the total angular momentum is compensated. At this point, the effective value of the gyromagnetic ratio  $\gamma$  diverges [11–13] as does the damping parameter  $\alpha$ , and, consequently, the character of the domain-wall motion changes from a precessionlike one [14] into that of Newtonian particles [7,15]. This happens because the absence of the angular momentum decouples the translational and precessional dynamics in the DW, leading to the disappearance of the Walker breakdown as well. It has been also experimentally verified that there is no DW magnetization tilt, and therefore no magnetic precession, at the angular momentum compensation [10]. In fact, early experiments on ferrimagnetic garnets directly demonstrated an increase of both the DW velocity and mobility [16–19]. Later, similar effects were also observed in (Gd, Fe)Co thin films in the vicinity of the angular momentum compensation temperature  $T_A$  [7], directly resembling the very fast dynamics expected in antiferromagnets. Thus ferrimagnets in the vicinity of their

\*andrei.kirilyuk@ru.nl

compensation point(s) seem to represent a golden compromise, where the accelerated dynamics is combined with ease of manipulation.

We should recall here, nevertheless, that a typical ferrimagnet can also possess a magnetization compensation point  $T_M$ , where the total magnetization of the sample becomes zero [20]. The separation between  $T_A$  and  $T_M$  depends on the ratio between the  $g$ -factors of two sublattices as well as on the properties of particular magnetic ions (see later discussion). At  $T_M$ , the loss of  $M$  is typically observed as the divergence of the coercive field, so that any manipulation of the magnetic order becomes very difficult at the very least. Because of this, there are hardly any data on the domain-wall dynamics in the vicinity of  $T_M$ , and nothing at all comparing the behavior at two compensation points directly.

While the direct applications of field-driven DW dynamics may be far off, there are still numerous applications of magnetic materials where the field-induced domain-wall motion constitutes an essential mechanism. These range from power transformers to magneto-optical modulators and to various concepts of data storage, including the “race-track” concepts solely controlled with magnetic fields [21]. Moreover, the understanding of the parameters defining the characteristics of DW motion plays the key role in the design of magnetic memory or logic elements. Nowadays, when the information density of magnetic data-storage media steadily increases and spintronic devices come in sight, a good understanding of the magnetic domain boundaries is of increasing technological relevance. Not only can the domain walls by themselves serve as magnetic bits, but it has been shown that the DWs can serve as broadband spin wave and elastic magnetization wave emitters [22]. DWs can be moved by magnetic fields, spin currents, temperature gradients, and short intense pulses of polarized light [23–25], as well as by indirect means such as pulsed anisotropy energy (see Ref. [26]). Of particular interest is also the behavior of DWs in nanostructures [27,28]. Experiments on the DW dynamics thus serve as a rich source of inspiration for various new concepts and devices, not only by themselves but also as an auxiliary tool for other purposes [29].

Here we present an experimental study of the domain-wall velocity in a ferrimagnetic garnet film in a wide temperature range, covering both  $T_M$  and  $T_A$  compensation points. This is made possible by the very low coercive field of the material, not exceeding 5 mT even in the close vicinity of  $T_M$ . A very unusual behavior of the domain-wall dynamics is observed, such as extraordinarily high mobility of the domain walls at very low fields, reaching Walker breakdown velocity  $v_W$  already at field values of less than 1–2 mT. It is shown that both  $v_W$  and the domain-wall mobility  $\mu$  vary by more than two orders of magnitude across a narrow temperature range of 70 K. Surprisingly,

the ratio of  $v_W$  and  $\mu$  is shown to vary in an essentially nonmonotonic way.

## II. EXPERIMENTAL DETAILS

The sample used in our experiments is a thin (thickness  $h = 3.1 \mu\text{m}$ ) film of magnetic garnet with a composition of  $(\text{Tm}, \text{Gd}, \text{Bi})_3(\text{Fe}, \text{Ga})_5\text{O}_{12}$ , deposited on a (111)-oriented substrate of lattice-matching gadolinium-gallium garnet using liquid-phase epitaxy. The magnetic anisotropy axis is perpendicular to the film plane. The iron ions exist in two different crystallographic positions and form two magnetic sublattices, oriented opposite to each other. The resulting ferrimagnetic moment is rather small and is strongly dependent on the Ga content, which preferably dilutes one of the sublattices. The intersublattice exchange interaction is sufficiently strong to make the garnet crystals ferrimagnetic up to temperatures of about 500 K. Relatively high Ga content in our case reduces the Curie temperature of our sample slightly to  $T_C = 445$  K.

The rare-earth (RE) part of the crystal is usually considered to be paramagnetic, but magnetized by the relatively weak interaction with the iron sublattices. This interaction is antiferromagnetic, and further (partially) compensates the total magnetic moment of the crystal. Depending on the exact composition, the considerably different temperature behavior of the ferromagnetlike Fe component and the quasiparamagnetic one of the RE component lead to a magnetic compensation point, in our case at  $T_M \approx 376$  K. The disappearance of the net magnetization of the sample at  $T_M$  makes the system insusceptible to an applied magnetic field.

Most interesting, however, is that due to the difference in the gyromagnetic ratios (e.g., the  $g$ -factors) of the two sublattices, a second compensation point appears—namely, that where the angular momenta of the sublattices are exactly compensated. In our case this occurs because of the mixture of two RE components, Gd with  $g \approx 2$  and Tm with  $g \approx 7/6$ . Thus, the effective  $g$ -factor for the RE system is expected to be considerably different from that of iron ( $g \approx 2$ ), and thus the temperature where the total angular momentum of the magnetic system vanishes ( $T_A$ ) will be different from  $T_M$ . This provides us with an interesting opportunity to investigate the magnetic dynamic behavior across both compensation points in comparison. In particular, the propagation of the domain wall is known to be strongly affected by the ratio of angular momentum to magnetic moments [8].

The magnetic hysteresis loops measured in Faraday geometry (see Fig. 1) directly reveal the magnetic compensation point  $T_M$  by three indications at once: a very sharp spike in coercivity as well as in the equilibrium size of domains, and a change in the sign of the Faraday effect. Also the shape of the loops is affected, due to the change in the ratio between anisotropy and demagnetizing field

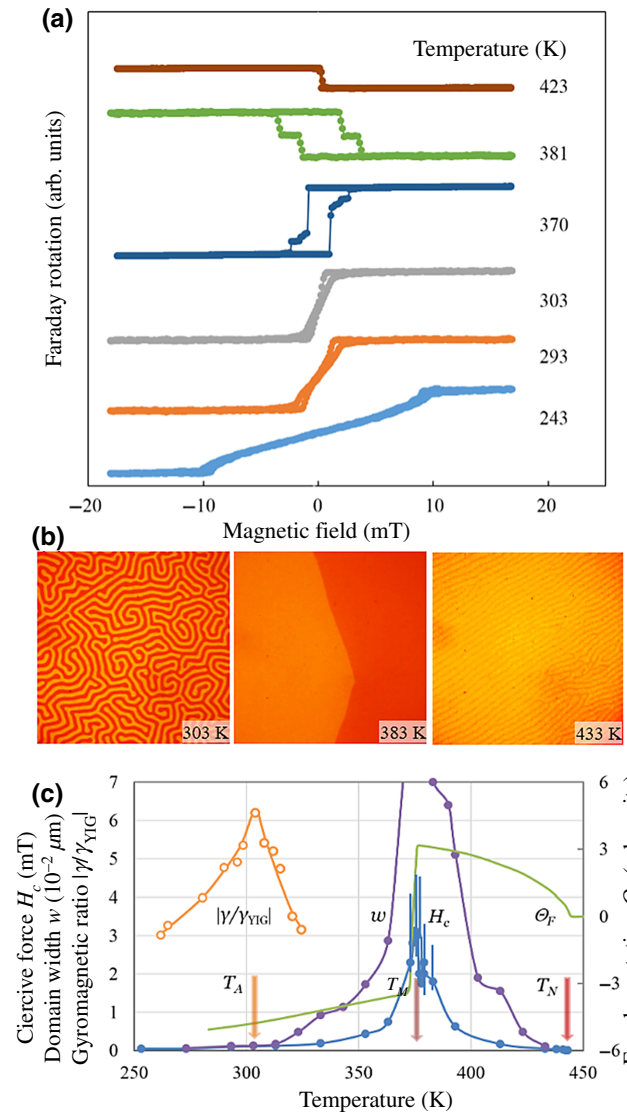


FIG. 1. (a) Static Faraday hysteresis loops showing the drastic change across the magnetic compensation temperature  $T_M \approx 376$  K; (b) equilibrium domain structures measured in zero applied magnetic field at different temperatures across  $T_M$ ; (c) coercive force  $H_c$ , equilibrium domain width  $w$ , absolute value of the gyromagnetic ratio for  $(\text{Tm}, \text{Gd}, \text{Bi})_3(\text{Fe}, \text{Ga})_5\text{O}_{12}$  relative to the gyromagnetic ratio for YIG  $|\gamma/\gamma_{\text{YIG}}|$ , and Faraday effect  $\Theta_F$  as a function of temperature in the vicinity of  $T_M$ ,  $T_A$ , and  $T_C$ .

values. The shape of the hysteresis curves in the vicinity of the compensation point could possibly be an indication of a spin-flop transition, as discussed before [30,31]. However, the present data do not allow for a definitive conclusion; moreover, we do not see any influence of this in the DW dynamics experiments. We thus leave the discussion of these loops out of the present paper. In contrast, the angular momentum compensation temperature  $T_A$  is not discovered in static measurements in any respect and only manifests itself in ferromagnetic resonance (FMR)

and dynamic experiments with domain wall motion (see below).

Note that the  $g$ -factors of Gd ( $g = 2$ ) and Tm ( $g = 7/6$ ) give an indication that the effective  $g$ -factor of the RE sublattice should be  $g_{\text{RE}} < 2 = g_{\text{Fe}}$ . Such a relation between  $g_{\text{RE}}$  and  $g_{\text{Fe}}$  suggests  $T_A > T_M$ . We shall see in the following, however, that the experiments show that the opposite is true. This is also confirmed by the results of measurements of the gyromagnetic ratio in the vicinity of the angular momentum compensation point  $T_A$  by the FMR technique using a Bruker ER200 spectrometer operating in the frequency range of 9.7 GHz (for more information, see the Appendix). In the immediate vicinity of  $T_A$ , the absolute value of the gyromagnetic ratio  $|\gamma|$  for  $(\text{Tm}, \text{Gd}, \text{Bi})_3(\text{Fe}, \text{Ga})_5\text{O}_{12}$  is more than 6 times the gyromagnetic ratio for yttrium iron garnet (YIG) [see Fig. 1(c)].

Next, we underline the very low coercive field of our sample, which stays below just a few tens of mT even in the close vicinity of  $T_M$ . This is clearly due to the very low number of magnetic defects in this material. Most important, this allows us to investigate the domain-wall dynamics in the full range of temperature across both compensation points.

To measure the propagation velocity of the domain walls, the following algorithm is used. Initially, the garnet film is nearly saturated by an applied bias field  $H_b$ , close to the saturation field  $H_s$ , and directed along the film normal. As a result, only a few small domains are left in the reversed state, as shown in white on the first image in Fig. 2. Typically, such residual domains can be assumed to correspond to certain inhomogeneities of the magnetic structure. Then, a pulse of magnetic field  $H_p$  directed opposite to the bias field  $H_b$  is applied to the sample, initiating the expansion of the white domains. The motion of the domain walls is recorded with the help of

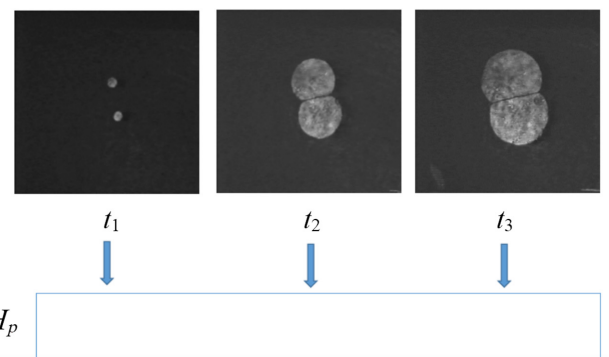


FIG. 2. The experimental scheme for the measurement of the domain-wall velocity, combining pulsed magnetic field  $H_p$  and 5-ns pulses of a laser for illumination. The images of the domain structures correspond to the time intervals  $t_1$ ,  $t_2$ , and  $t_3$  from the start of the magnetic field pulse.

a single-shot photography technique, using 5-ns-long laser pulses for illumination. Note that a single image is taken for each applied magnetic field pulse. Changing the delay between the field and laser pulses allows us to obtain sequential images of the domain-wall position during its motion. We thus can observe the domain-wall position at various times  $t_i$  after the beginning of the magnetic field pulse, selected such that the interval  $\Delta t$  between them stays constant:  $\Delta t = t_1 - t_2 = t_2 - t_3$  and so on (see Fig. 2). Such an approach guarantees the reproducibility of measurements, as the sequential images show different stages of the domain-wall motion started from the same initial position.

Typically, the duration of the magnetic field pulses is 2–5  $\mu$ s, with a rise time of only 5 ns. As the domain-wall velocity varies by more than 2 orders of magnitude (see Fig. 3), the time interval  $\Delta t$  is varied from 20 ns to 1  $\mu$ s. This is done to keep the corresponding distance covered by the domain wall of the order to several tens of micrometers, such that it would be straightforward to precisely measure it with the help of a polarizing microscope.

### III. RESULTS

Typically, at low magnetic fields, the field-driven propagation of domain walls occurs with their velocity proportional to the magnetic field value:  $v = \mu H$ , where  $\mu$  is the domain-wall mobility. This regime is limited from above by the so-called Walker velocity limit  $v_W$ , after which the domain-wall motion becomes spatially and temporally inhomogeneous.

However, the typical dependencies of the DW velocity on the applied magnetic field measured in our system show quite a different behavior (see Fig. 3). In fact, the majority of the curves show a sizable offset  $v_{\text{off}}$  of the velocity at  $H \cong 0$ , followed by what can be interpreted as linear behavior of the expected type  $\Delta v = \mu_{\text{eff}}H$ . Such an offset is very unusual and can be interpreted in the following way.

Because of the very high domain-wall mobility  $\mu$  for the initial part of the dependence of its velocity on the applied magnetic field  $v(H)$ , already in magnetic fields of some 0.5–1.5 mT, we cross the Walker limit velocity and enter a different regime. Unfortunately, we are not able to study this initial regime because of domain-wall magneto-static instabilities: for a small value of the driving field  $H$ , domain scattering fields compete with it [14]. As a result, the propagation of domain walls becomes uneven and the shape of the walls is distorted. We therefore define the domain-wall velocity observed for the driving magnetic field of  $H_{\text{cr}} = 2$  mT as the offset velocity  $v_{\text{off}}$ . After such an offset, a linear behavior  $v(H)$  is observed (see Fig. 3), which could be characterized by the effective domain-wall mobility  $\mu_{\text{eff}}$  as  $v(H) = v_{\text{off}} + \mu_{\text{eff}}H$ . According to the one-dimensional theory of the domain-wall dynamics [14], such mobility in magnetic fields much larger than the Walker limit is given by

$$\mu_{\text{eff}} = \frac{\mu\alpha^2}{1 + \alpha^2}, \quad (1)$$

where  $\alpha$  is the Gilbert damping constant. Thus, even with a relatively high value of  $\alpha = 0.1$  one obtains  $\mu_{\text{eff}}/\mu = 0.01$ . In other words, the observed linear dependence of domain-wall velocity as a function of the applied magnetic field (Fig. 3) is actually given by the time-averaged inhomogeneous motion above the Walker limit.

The two main parameters of  $\mu_{\text{eff}}$  and  $v_{\text{off}}$  that characterize the domain-wall dynamics for the garnet are thus investigated in a broad temperature range covering all critical points of the sample, namely  $T_M$ ,  $T_A$ , and  $T_C$ . Both the mobility and velocity offset reach maximum at the angular momentum compensation point, exceeding by more than 2 orders of magnitude the corresponding values observed at the magnetic compensation temperature.

Already Fig. 3 shows us that to some extent, the values of  $\mu_{\text{eff}}$  and  $v_{\text{off}}$  can vary independently of each other. Thus, Fig. 3(a) shows that the offset velocity  $v_{\text{off}}$  changes

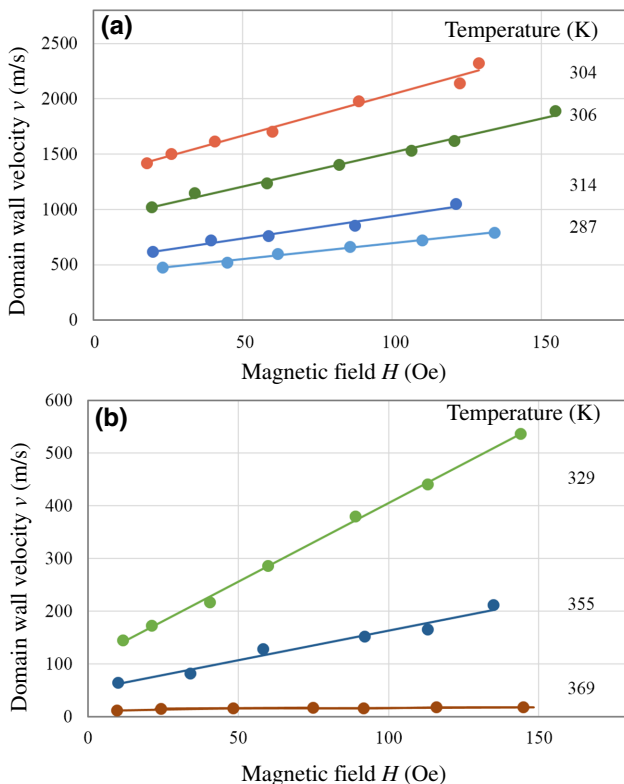


FIG. 3. The dependencies of the domain-wall velocity as a function of applied magnetic field  $v(H)$  are shown for a number of temperatures, split in two temperature regions: (a) strong change of the offset velocity  $v_{\text{off}}$  with almost constant mobility, in the vicinity of  $T_A$ , and (b) small changes of  $v_{\text{off}}$  with a strong change of mobility close to the magnetic compensation point  $T_M$ .

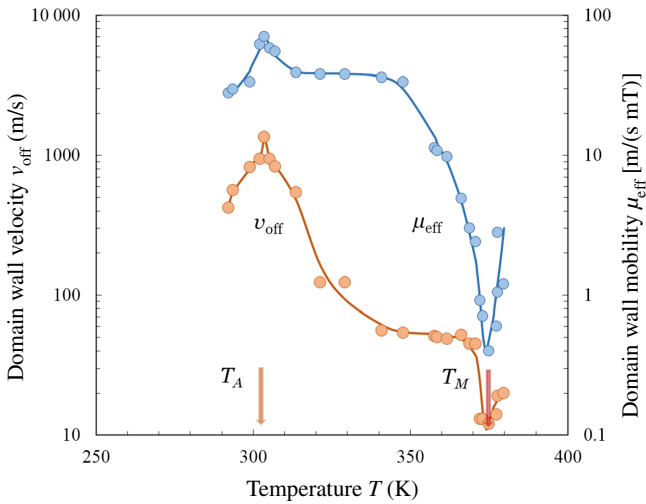


FIG. 4. The derived values of effective domain-wall mobility  $\mu_{\text{eff}}$  and offset velocity  $v_{\text{off}}$  as a function of temperature.

10 times in the temperatures range of  $T = 315\text{--}345$  K, while the mobility  $\mu_{\text{eff}}$  stays nearly constant. In contrast, in the narrow range of  $T = 353\text{--}365$  K we observe a steep decrease of the mobility toward the compensation point  $T_M$ , whereas the offset velocity hardly changes.

Having assumed this, in the following we characterize the measured dependencies with the parameters  $\mu_{\text{eff}}$  and  $v_{\text{off}}$ , obtained from the fitting of the measured dependencies  $v(H)$  by the linear formula  $v(H) = v_{\text{off}} + \mu_{\text{eff}}H$ . The resulting values are shown in Fig. 4 as a function of temperature. Note that a logarithmic scale is used. Figure 4 clearly shows the two compensation points as sharp minima of both observables at  $T_M$ , and almost equally sharp maxima at  $T_A$ . Note that this measurement is the only one that indicates the position of the angular momentum compensation point (along with the FMR data; see Figs. 1 and 6), as there is no sign of it in any of the static parameters.

An important point that should be mentioned here is that in ferromagnets, typically the temperature dependence of the domain-wall mobility is given by  $\mu \propto T^{-2}$ , obtained from four-magnon scattering [14]. In our case, however, the whole considered temperature interval is small enough, so that such dependence can practically be ignored as compared with the changes of more than 2 orders of magnitude introduced by the presence of the compensation points. To understand the dynamics of domain walls, the question of wall structure is crucial. If the initial structure of the domain wall is simple and does not contain Bloch lines, the domain wall moves uniformly in small magnetic fields  $H$  and its velocity is proportional to the magnetic field [3]. In a magnetic field exceeding the critical value, the stationary motion of the wall is disrupted and the domain wall is divided into sections with different directions of magnetization vector twisting. According to the one-dimensional

theory of domain-wall dynamics, the domain-wall velocity is limited by the Walker velocity [32]:

$$v_W = \gamma \sqrt{\frac{\mu_0 A}{2Q}}, \quad (2)$$

where  $A$  is the exchange constant,  $Q = 2K_u/(\mu_0 M_s^2)$  the quality factor of uniaxial magnetic material,  $K_u$  the constant of uniaxial magnetic anisotropy,  $\mu_0$  the magnetic permeability of free space, and  $M_s$  the saturation magnetization.

Despite the development of more accurate two- and three-dimensional models [8,14], the one-dimensional model remains the most popular one, which is customarily used to compare experimental results. For our case, near  $T_A \approx 303$  K, the parameters of the  $(\text{Tm}, \text{Gd}, \text{Bi})_3(\text{Fe}, \text{Ga})_5\text{O}_{12}$  sample are  $Q \approx 18$  and  $A \approx 2.2 \times 10^{-12}$  J/m. The gyromagnetic ratio  $\gamma \rightarrow \infty$  at the angular momentum compensation point, and in real materials  $\gamma$  can increase up to 30 times [16–19,33] compared with the gyromagnetic ratio for a free electron. Accordingly, the Walker velocity limit will be  $v_W \approx 1500$  m/s, which is well in agreement with the experimental data (see Fig. 4).

In the vicinity of the magnetic momentum compensation point, we observe a sharp dip in the dependence of the velocity on the field (Fig. 4), where the DW velocity value drops by 2 orders of magnitude compared to the velocity when the angular momentum is compensated. Near  $T_M$ , the field-induced torques that are proportional to the magnetization vanish, which thus leads to the observed drop of the DW velocity. It is interesting to note that in the experiments on the DW motion driven by spin-polarized currents in GdCo [15], there was no visible effect of  $T_M$  on the DW dynamics, in strong contrast to our case. This is possibly caused by the fundamental difference between the field-induced torques, acting on the net magnetization of the system, and the current-induced ones that predominantly affect the transition-metal sublattice and thus would be less sensitive to the magnetization compensation.

To further confirm our experimental results, we can compare them with quantitative estimates obtained from a well-developed mathematical model [8] for the dynamics of DWs in ferrimagnets. According to the sigma-model of a two-sublattice ferrimagnet with spin densities  $s_{1,2}$ , the maximum DW velocity  $v$  can be found:

$$v = \frac{v_W c}{\sqrt{v_W^2 + c^2}}, \quad (3)$$

where  $v_W = [\sqrt{AK}/\hbar(s_1 - s_2)](\sqrt{1 + \rho} - 1)$  is the Walker limiting velocity and  $c = \sqrt{A\omega_{\text{ex}}/\hbar(s_1 + s_2)}$  is the minimum spin-wave velocity, which is determined by the exchange interaction with homogeneous and

inhomogeneous exchange constants  $E_{\text{ex}}$  and  $A$ , respectively. Here  $\omega_{\text{ex}} = E_{\text{ex}}/\hbar(s_1 + s_2)$  is the characteristic exchange frequency,  $K$  is the uniaxial anisotropy constant, and  $\rho = K_p/K$  is a small parameter, where  $K_p$  describes the small effective anisotropy field in the basis plane. At the angular momentum compensation point,  $s_1 \approx s_2$  and the maximum DW velocity is equal to  $c$ . For  $\omega_{\text{ex}} \approx 10^{13} \text{ s}^{-1}$  and  $s_i = M_i/g_i\mu_B$  [6,12], with  $i = 1, 2$ , we find  $c \approx 1500 \text{ m/s}$ , which is well in agreement with the experimental data (see Fig. 4).

#### IV. DISCUSSION

Let us first briefly recap what should actually be expected from the domain wall behavior at temperatures close to the compensation points. First, at the magnetization compensation point  $T_M$ , the susceptibility of the system to the applied magnetic field vanishes. In statics this is directly revealed by a sharp increase of the coercive field accompanied by a similarly sharp increase of the equilibrium size of magnetic domains; in addition, the sign of the Faraday effect changes (the direction of Larmor precession changes when passing through the point of magnetic moment compensation), while its modulus remains stable (see Fig. 1). In agreement with the reduction of susceptibility, our data show a very sharp drop (though not to zero) of both the offset velocity  $v_{\text{off}}$  as well as the domain-wall mobility  $\mu_{\text{eff}}$  (Fig. 4).

In contrast, at the angular momentum compensation temperature  $T_A$ , static susceptibility of the system is not affected: a finite magnetization  $M$  is present, and the static hysteresis loops show a very smooth variation across, without any features. However, this point becomes directly visible in dynamics measurements (see Ref. [20]). The absence of the angular momentum makes the magnetic resonance frequency approach that of a typical antiferromagnet [34]. In our measurements, a very sharp increase of both the domain-wall velocity and mobility is detected. This is in agreement both with expectations and with other data.

An interesting point is that from the macrospin consideration, the effective damping parameter  $\alpha$  diverges at the angular momentum compensation point [20,35]. While this has been confirmed by some experiments [36], others have shown a complete independence of damping on temperature in the region of  $T_A$  [13]. Also related to the rare-earth-transition-metal alloys, the increase of  $\alpha$  was found in all-optical FMR experiments [20,37] but not in the domain-wall mobility [38]. The fact that the macrospin treatment is not in agreement with the observed increase of the domain-wall mobility at  $T_A$  once again confirms the dominance of the multisublattice character of the domain-wall dynamics in compensated ferrimagnets. We thus leave this question open for further research.

In between the two compensation points, the offset velocity  $v_{\text{off}}$  and the domain mobility  $\mu_{\text{eff}}$  show rather independent behavior. This we can tentatively relate to the ratio between the magnetic moment and the angular momentum of the system in this region.

The last point that needs to be discussed here is the location of the angular momentum compensation point  $T_A$ . In a recent publication [39] it has been discussed how one can estimate the difference  $\Delta T$  between the two compensation points, which, in our case, would predict  $T_A$  to be above  $T_M$ . However, while the approach of Ref. [39], which is roughly based on the original proposal of Wangsness [11], may be applicable to the (Gd,Fe)Co alloys, the situation is different for garnet with other rare-earth elements. After the work of Wangsness, Kittel argued that the rare-earth metals with nonzero orbital moment are heavily damped, and “the damped lattice contributes fully to the magnetization but not to the angular momentum density... The RE system, being highly damped, does not respond to an applied torque as a normal gyroscopic system. We may think of the angular momentum of the RE system as largely imaginary” [12]. In the subsequent work of van Vleck, the rare-earth ions were treated as captive in the exchange field from iron, but subject to decomposition of their energy levels by crystalline fields and/or spin-orbit interaction [40]. He showed that in the case of Gd, crystal field is negligible as compared to the exchange field, and the result is that of Wangsness. For the other rare-earth metals, with large crystal-field decomposition, the result of van Vleck becomes equivalent to that of Kittel. While the starting points of Kittel and van Vleck seem rather different, the latter also admits that “in a certain sense, however, the difference between our theory and Kittel’s is a semantic one.” Therefore, excluding the contribution of Tm sublattice from the angular momentum sum shifts  $T_A$  to lower temperature. Note that a very similar system, also containing Gd and Tm, was treated both experimentally (FMR) and theoretically (molecular field theory of Néel [41]; see also Ref. [42]) in Ref. [19]. A good correspondence was found, confirming the validity of such an approach. In our work, therefore, we limit ourselves to finding  $T_A$  by FMR measurements; see data in Fig. 1(c) and the Appendix.

#### V. CONCLUSIONS

To summarize, the weak coercive field of our sample combined with the high mobility of domain walls allows us to study in detail the domain-wall dynamics across both magnetic and angular momentum compensation points. Drastic changes of both domain-wall velocity and mobility by more than 2 orders of magnitude are observed across a relatively small temperature range, related to the delicate balance of magnetization and spins of iron and rare-earth

sublattices. Therefore, such fine tuning of the corresponding momenta could be the key for developing ultrafast ferrimagnetic spintronic devices.

### ACKNOWLEDGMENTS

We would like to acknowledge the support of Russian Foundation for Basic Research (Projects No. 18-29-27020 and No. 18-52-16006), Russian Science Foundation (Grant No. 19-19-00607), and a grant from the Government of the Russian Federation for state support of scientific research conducted under the guidance of leading scientists in Russian higher education institutions, research institutions, and state research centers of the Russian Federation (Project No. 075-15-2019-1874). We also would like to acknowledge networking support by the COST Action No. CA17123 “Ultrafast opto magneto electronics for nondissipative information technology.” A.R. acknowledges the support from the RFBR (Grant No. 19-29-03015) and a grant of the President of the Russian Federation (Grant No. MK-283.2019.8). S.A. acknowledges support from the Government of the Russian Federation (Grant No. 074-02-2018-286 for the “Terahertz Spintronics” laboratory of the MIPT).

### APPENDIX: MEASUREMENTS OF TEMPERATURE DEPENDENCE OF THE GYROMAGNETIC RATIO BY FMR

The magnetic resonance behavior of the garnet film used with composition  $(\text{Tm}, \text{Gd}, \text{Bi})_3(\text{Fe}, \text{Ga})_5\text{O}_{12}$  is measured using a Bruker ER200 spectrometer at a set frequency of 9.7 GHz. The scanning range of the magnetic field of the spectrometer is 10–800 mT, which makes it possible to measure the effective ferromagnetic mode. During the measurements, FMR is recorded with the magnetic field applied both in the film plane as well as perpendicular to the film plane. The observed FMR signals show no special features and just a single resonance peak (see Fig. 5). Note that an extra feature of very small amplitude might be inferred at low field values and in the vicinity of the compensation temperature. While this might be a fingerprint of the ferrimagnetic mode, the signal-to-noise ratio of our spectrometer does not allow for any definitive conclusions. We therefore limit our consideration to the essential for our purposes FMR signal.

When approaching the angular momentum compensation temperature, the resonant field for the geometry with the applied field perpendicular to the film surface goes beyond the range of our spectrometer, and the data for the gyromagnetic ratio [see Fig. 1(c)] are calculated using the FMR data obtained in the in-plane field geometry (Fig. 6). Well-known equations are used for the gyromagnetic ratio calculation, see Ref. [43], taking into account the uniaxial

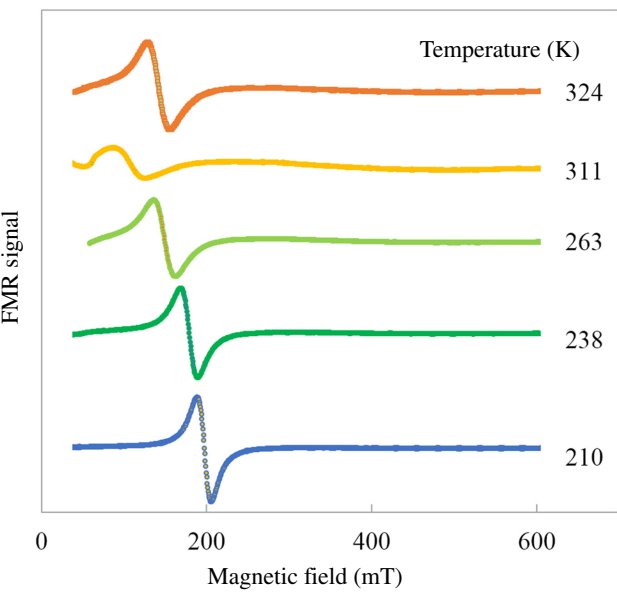


FIG. 5. FMR signals for the effective ferromagnetic mode below and above the angular momentum compensation temperature  $T_A = 305$  K as a function of the in-plane applied magnetic field.

anisotropy of the film that was measured before by a magneto-optical method [44]. The method allows us to measure the constants of uniaxial, cubic, and rhombic anisotropy components at an arbitrary ratio between them. In brief, the method is based on the measurement of the orientational dependencies of Faraday rotation in magnetic fields applied approximately parallel to the film surface. In these measurements, the magnetic field strength significantly exceeds the strength of the effective magnetic anisotropy field [44].

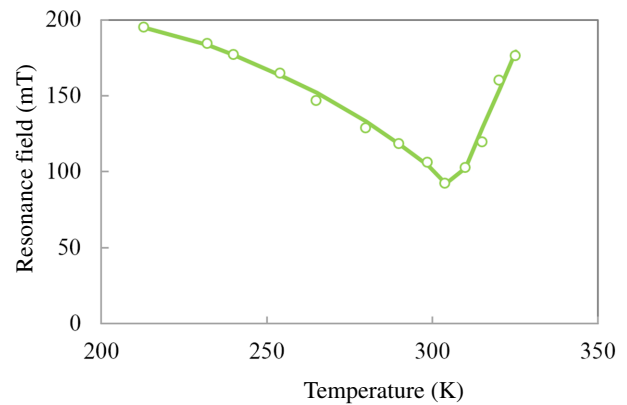


FIG. 6. FMR fields for the effective ferromagnetic mode in the vicinity of the angular momentum compensation temperature  $T_A = 305$  K of the ferrimagnetic sample, where the resonant field has a minimum. The magnetic field is applied parallel to the film plane.

- [1] T. Jungwirth, X. Marti, P. Wadley, and J. Wunderlich, Antiferromagnetic spintronics, *Nat. Nanotechnol.* **11**, 231 (2016).
- [2] V. Baltz, A. Manchon, M. Tsoi, T. Moriyama, T. Ono, and Y. Tserkovnyak, Antiferromagnetic spintronics, *Rev. Mod. Phys.* **90**, 015005 (2018).
- [3] L. D. Landau, *Electrodynamics of Continuous Media* (Butterworth-Heinemann, Oxford England, 1984).
- [4] S. V. Vonsovskii, *Magnetism* (J. Wiley, New York, 1974).
- [5] S. Konishi, T. Miyama, and K. Ikeda, Domain wall velocity in orthoferrites, *Appl. Phys. Lett.* **27**, 258 (1975).
- [6] V. G. Baryakhtar, B. A. Ivanov, and Mikhail V. Chetkin, Dynamics of domain walls in weak ferromagnets, *Usp. Fiz. Nauk* **146**, 417 (1985).
- [7] Kab-Jin Kim, Se Kwon Kim, Yuushou Hirata, Se-Hyeok Oh, Takayuki Tono, Duck-Ho Kim, Takaya Okuno, Woo Seung Ham, Sanghoon Kim, Gyoungchoon Go, Yaroslav Tserkovnyak, Arata Tsukamoto, Takahiro Moriyama, Kyung-Jin Lee, and Teruo Ono, Fast domain wall motion in the vicinity of the angular momentum compensation temperature of ferrimagnets, *Nat. Mater.* **16**, 1187 (2017).
- [8] B. A. Ivanov, Ultrafast spin dynamics and spintronics for ferrimagnets close to the spin compensation point (review), *Low Temp. Phys.* **45**, 935 (2019).
- [9] Joseph Finley and Luqiao Liu, Spintronics with compensated ferrimagnets, *Appl. Phys. Lett.* **116**, 110501 (2020).
- [10] E. Haltz, J. Sampaio, S. Krishnia, L. Berge, R. Weil, and A. Mougin, Measurement of the tilt of a moving domain wall shows precession-free dynamics in compensated ferrimagnets, *Sci. Rep.* **10**, 16292 (2020).
- [11] Roald K. Wangsness, Sublattice effects in magnetic resonance, *Phys. Rev.* **91**, 1085 (1953).
- [12] C. Kittel, Theory of ferromagnetic resonance in rare earth garnets. I. *g* values, *Phys. Rev.* **115**, 1587 (1959).
- [13] R. C. LeCraw, J. P. Remeika, and H. Matthews, Angular momentum compensation in narrow linewidth ferrimagnets, *J. Appl. Phys.* **36**, 901 (1965).
- [14] A. P. Malozemoff and J. C. Slonczewski, *Magnetic Domain Walls in Bubble Materials* (Academic Press, New York, 1979).
- [15] Lucas Caretta, Maxwell Mann, Felix Büttner, Kohei Ueda, Bastian Pfau, Christian M. Günther, Piet Hessing, Alexandra Churikova, Christopher Klose, Michael Schneider, Dieter Engel, Colin Marcus, David Bono, Kai Babschik, Stefan Eisebitt, and Geoffrey S. D. Beach, Fast current-driven domain walls and small skyrmions in a compensated ferrimagnet, *Nat. Nanotechnol.* **13**, 1154 (2018).
- [16] G. P. Vella-Coleiro, S. L. Blank, and R. C. LeCraw, Influence of gyromagnetic ratio on magnetic domain wall dynamics, *Appl. Phys. Lett.* **26**, 722 (1975).
- [17] R. C. LeCraw, S. L. Blank, and G. P. Vella-Coleiro, New high-speed bubble garnets based on large gyromagnetic ratios (high *g*), *Appl. Phys. Lett.* **26**, 402 (1975).
- [18] Norio Ohta, Tadashi Ikeda, Fumihiro Ishida, and Yutaka Sugita, High *g* bubble garnets without containing Eu<sup>3+</sup> ion, *J. Phys. Soc. Jpn.* **43**, 705 (1977).
- [19] N. A. Loginov, M. V. Logunov, and V. V. Randoshkin, Properties of (Gd, Tm, Bi)<sub>3</sub>(Fe, Ga)<sub>5</sub>O<sub>12</sub> films in the vicinity of the angular momentum compensation point, Sov. Phys. Solid State **31**, 1684 (1989).
- [20] C. D. Stanciu, A. V. Kimel, F. Hansteen, A. Tsukamoto, A. Itoh, A. Kirilyuk, and Th. Rasing, Ultrafast spin dynamics across compensation points in ferrimagnetic GdFeCo: The role of angular momentum compensation, *Phys. Rev. B* **73**, 220402 (2006).
- [21] Fanny Ummelen, Henk Swagten, and Bert Koopmans, Racetrack memory based on in-plane-field controlled domain-wall pinning, *Sci. Rep.* **7**, 833 (2017).
- [22] R. B. Holländer, C. Müller, J. Schmalz, M. Gerken, and J. McCord, Magnetic domain walls as broadband spin wave and elastic magnetisation wave emitters, *Sci. Rep.* **8**, 13871 (2018).
- [23] M. V. Gerasimov, M. V. Logunov, A. V. Spirin, Yu N. Nozdrin, and I. D. Tokman, Time evolution of domain-wall motion induced by nanosecond laser pulses, *Phys. Rev. B* **94**, 014434 (2016).
- [24] R. Medapalli, D. Afanasiev, D. K. Kim, Y. Quessab, S. Manna, A. Montoya, A. Kirilyuk, Th. Rasing, A. V. Kimel, and E. E. Fullerton, Multiscale dynamics of helicity-dependent all-optical magnetization reversal in ferromagnetic Co/Pt multilayers, *Phys. Rev. B* **96**, 224421 (2017).
- [25] G. Kichin, M. Hehn, J. Gorchon, G. Malinowski, J. Hohlfeld, and S. Mangin, From Multiple- to Single-Pulse All-Optical Helicity-Dependent Switching in Ferromagnetic Co/Pt Multilayers, *Phys. Rev. Appl.* **12**, 024019 (2019).
- [26] A. W. Rushforth, R. Rowan-Robinson, and Zemen J, Deterministic magnetic domain wall motion induced by pulsed anisotropy energy, *J. Phys. D: Appl. Phys.* **53**, 164001 (2020).
- [27] L. Herrera Diez, F. Ummelen, V. Jeudy, G. Durin, L. Lopez-Diaz, R. Diaz-Pardo, A. Casiraghi, G. Agnus, D. Bouville, J. Langer, B. Ocker, R. Lavrijsen, H. J. M. Swagten, and D. Ravelosona, Magnetic domain wall curvature induced by wire edge pinning, *Appl. Phys. Lett.* **117**, 062406 (2020).
- [28] J. A. Fernandez-Roldan, A. De Riz, B. Trapp, C. Thirion, M. Vazquez, J.-C. Toussaint, O. Fruchart, and D. Gusakova, Modeling magnetic-field-induced domain wall propagation in modulated-diameter cylindrical nanowires, *Sci. Rep.* **9**, 5130 (2019).
- [29] Xueying Zhang, Nicolas Vernier, Laurent Vila, Shao-hua Yan, Zhiqiang Cao, Anni Cao, Zili Wang, Wen-long Cai, Yang Liu, Huaiwen Yang, Dafiné Ravelosona, and Weisheng Zhao, Low Spin Polarization in Heavy-Metal–Ferromagnet Structures Detected Through Domain-Wall Motion by Synchronized Magnetic Field and Current, *Phys. Rev. Appl.* **11**, 054041 (2019).
- [30] J. Becker, A. Tsukamoto, A. Kirilyuk, J. C. Maan, Th. Rasing, P. C. M. Christianen, and A. V. Kimel, Ultrafast Magnetism of a Ferrimagnet across the Spin-Flop Transition in High Magnetic Fields, *Phys. Rev. Lett.* **118**, 117203 (2017).
- [31] A. M. Kalashnikova, V. V. Pavlov, A. V. Kimel, A. Kirilyuk, Th. Rasing, and R. V. Pisarev, Magneto-optical study of holmium iron garnet Ho<sub>3</sub>Fe<sub>5</sub>O<sub>12</sub>, *Low Temp. Phys.* **38**, 863 (2012).
- [32] George Rado, *Magnetism: A Treatise on Modern Theory and Materials* (Academic Press, New York, London, 1963).
- [33] N. A. Loginov, M. V. Logunov, and V. V. Randoshkin, Symbol of efficient magnitude of gyromagnetic ratio in

- ferrite-garnet films near the point of pulse moment compensation, *Zh. Tekh. Fiz.* **60**, 126 (1990).
- [34] A. G. Gurevich, *Magnetization Oscillations and Waves* (CRC Press, Boca Raton, Florida, 1996).
- [35] Masud Mansuripur, *The Physical Principles of Magneto-Optical Recording* (Cambridge University Press, Cambridge, England, 1995).
- [36] B. A. Calhoun, J. Overmeyer, and W. V. Smith, Ferrimagnetic resonance in gadolinium iron garnet, *Phys. Rev.* **107**, 993 (1957).
- [37] M. Binder, A. Weber, O. Mosendz, G. Woltersdorf, M. Izquierdo, I. Neudecker, J. R. Dahn, T. D. Hatchard, J.-U. Thiele, C. H. Back, and M. R. Scheinfein, Magnetization dynamics of the ferrimagnet CoGd near the compensation of magnetization and angular momentum, *Phys. Rev. B* **74**, 134404 (2006).
- [38] Duck-Ho Kim, Takaya Okuno, Se Kwon Kim, Se-Hyeok Oh, Tomoe Nishimura, Yuushou Hirata, Yasuhiro Futakawa, Hiroki Yoshikawa, Arata Tsukamoto, Yaroslav Tserkovnyak, Yoichi Shiota, Takahiro Moriyama, Kab-Jin Kim, Kyung-Jin Lee, and Teruo Ono, Low Magnetic Damping of Ferrimagnetic GdFeCo Alloys, *Phys. Rev. Lett.* **122**, 127203 (2019).
- [39] Yuushou Hirata, Duck-Ho Kim, Takaya Okuno, Tomoe Nishimura, Dae-Yun Kim, Yasuhiro Futakawa, Hiroki Yoshikawa, Arata Tsukamoto, Kab-Jin Kim, Sug-Bong Choe, and Teruo Ono, Correlation between compensation temperatures of magnetization and angular momentum in GdFeCo ferrimagnets, *Phys. Rev. B* **97**, 220403(R) (2018).
- [40] J. H. van Vleck, Primitive theory of ferrimagnetic resonance frequencies in rare-earth iron garnets, *Phys. Rev.* **123**, 58 (1961).
- [41] L. Néel, Propriétés magnétiques des ferrites; ferrimagnétisme et antiferromagnétisme, *Am. Phys.* **12**, 137 (1948).
- [42] C. D. Brandle and S. L. Blank, Magnetic moments for mixed substituted rare earth iron garnets, *IEEE Trans. Magn. MAG-12*, 14 (1976).
- [43] A. Gangulee and R. J. Kobliska, Magnetocrystalline anisotropy in epitaxially grown  $(\text{Gd}, \text{Tm}, \text{Y})_3(\text{Fe}, \text{Ga})_5\text{O}_{12}$  garnet thin films, *J. Appl. Phys.* **51**, 3333 (1980).
- [44] A. M. Balbashov, I. E. Dikshtein, F. V. Lisovskii, E. G. Mansvetova, L. M. Filimonova, and E. S. Chizhik, Determining the anisotropy constants of ferrite garnets with an arbitrary ratio of the contributions of uniaxial, cubic, and rhombic components, *Sov. Microelectron.* **20**, 45 (1990).